

Extracardiac conduit adequacy along the respiratory cycle in adolescent Fontan patients

Rijnberg, Friso M.; Van Der Woude, Séline F.S.; Hazekamp, Mark G.; Van Den Boogaard, Pieter J.; Lamb, Hildo J.; Terol Espinosa De Los Monteros, Covadonga; Kenjeres, Sasa; Karim, Tawab; Jongbloed, Monique R.M.; More Authors

DOI

[10.1093/ejcts/ezab478](https://doi.org/10.1093/ejcts/ezab478)

Publication date

2022

Document Version

Final published version

Published in

European Journal of Cardio-thoracic Surgery

Citation (APA)

Rijnberg, F. M., Van Der Woude, S. F. S., Hazekamp, M. G., Van Den Boogaard, P. J., Lamb, H. J., Terol Espinosa De Los Monteros, C., Kenjeres, S., Karim, T., Jongbloed, M. R. M., & More Authors (2022). Extracardiac conduit adequacy along the respiratory cycle in adolescent Fontan patients. *European Journal of Cardio-thoracic Surgery*, 62(1), Article ezab478. <https://doi.org/10.1093/ejcts/ezab478>

Important note

To cite this publication, please use the final published version (if applicable).
Please check the document version above.

Copyright





Other than for strictly personal use, it is not permitted to download, forward or distribute the text or part of it, without the consent of the author(s) and/or copyright holder(s), unless the work is under an open content license such as Creative Commons.

Takedown policy

Please contact us and provide details if you believe this document breaches copyrights.
We will remove access to the work immediately and investigate your claim.

Cite this article as: Rijnberg FM, van der Woude SFS, Hazekamp MG, van den Boogaard PJ, Lamb HJ, Terol Espinosa de Los Monteros C *et al.* Extracardiac conduit adequacy along the respiratory cycle in adolescent Fontan patients. *Eur J Cardiothorac Surg* 2022; doi:10.1093/ejcts/ezab478.

Extracardiac conduit adequacy along the respiratory cycle in adolescent Fontan patients

Friso M. Rijnberg ^{a,*}, Séline F.S. van der Woude^b, Mark G. Hazekamp ^a, Pieter J. van den Boogaard^c, Hildo J. Lamb^c, Covadonga Terol Espinosa de Los Monteros^d, Lucia J.M. Kroft^c, Sasa Kenjeres^e, Tawab Karim^b, Monique R.M. Jongbloed^f, Jos J.M. Westenberg ^c, Jolanda J. Wentzel^b and Arno A.W. Roest ^d

^a Department of Cardiothoracic Surgery, Leiden University Medical Center, Leiden, Netherlands

^b Department of Cardiology, Biomechanical Engineering, Erasmus MC, Rotterdam, Netherlands

^c Department of Radiology, Leiden University Medical Center, Leiden, Netherlands

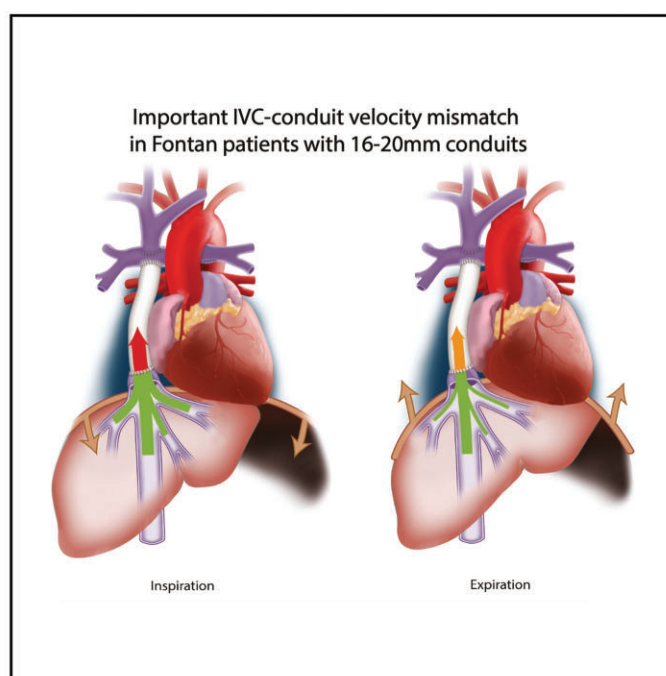
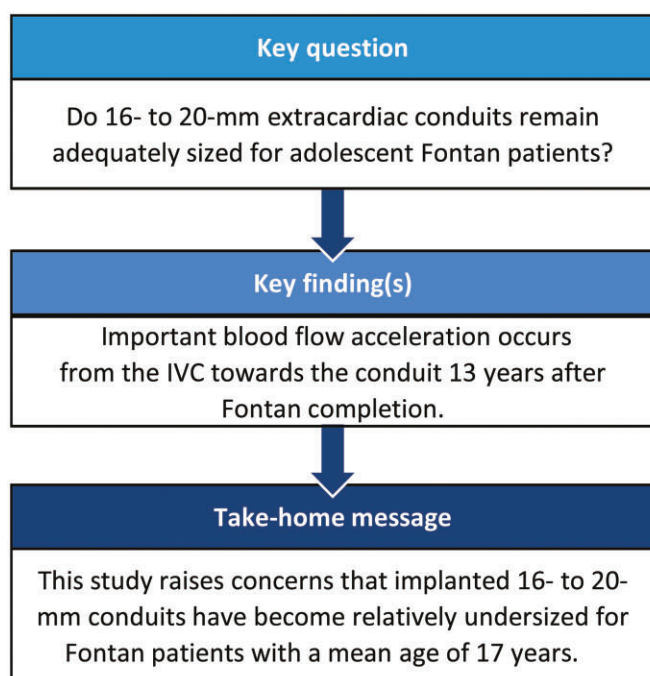
^d Department of Pediatric Cardiology, Leiden University Medical Center, Leiden, Netherlands

^e Department of Chemical Engineering, Faculty of Applied Sciences, Delft University of Technology and J.M. Burgers Centrum Research School for Fluid Mechanics, Delft, Netherlands

^f Department of Cardiology and Anatomy and Embryology, Leiden University Medical Center, Leiden, Netherlands

* Corresponding author. Department of Cardiothoracic surgery, Leiden University Medical Center, Albinusdreef 2, Leiden 2333 ZA, Netherlands. Tel: +31-715262348; e-mail: f.m.rijnberg@lumc.nl (F.M. Rijnberg).

Received 5 July 2021; received in revised form 12 September 2021; accepted 26 September 2021



Abstract

OBJECTIVES: Adequacy of 16–20mm extracardiac conduits for adolescent Fontan patients remains unknown. This study aims to evaluate conduit adequacy using the inferior vena cava (IVC)–conduit velocity mismatch factor along the respiratory cycle.

Presented at the 35th Annual Meeting of the European Association for Cardio-Thoracic Surgery, Barcelona, Spain, 13–16 October 2021.

METHODS: Real-time 2D flow MRI was prospectively acquired in 50 extracardiac (16–20mm conduits) Fontan patients (mean age 16.9 ± 4.5 years) at the subhepatic IVC, conduit and superior vena cava. Hepatic venous flow was determined by subtracting IVC flow from conduit flow. The cross-sectional area (CSA) was reported for each vessel. Mean flow and velocity was calculated during the average respiratory cycle, inspiration and expiration. The IVC–conduit velocity mismatch factor was determined as follows: $V_{\text{conduit}}/V_{\text{IVC}}$, where V is the mean velocity.

RESULTS: Median conduit CSA and IVC CSA were 221 mm^2 (Q1–Q3 201–255) and 244 mm^2 (Q1–Q3 203–265), respectively. From the IVC towards the conduit, flow rates increased significantly due to the entry of hepatic venous flow (IVC 1.9, Q1–Q3 1.5–2.2) versus conduit (3.3, Q1–Q3 2.5–4.0 l/min, $P < 0.001$). Consequently, mean velocity significantly increased (IVC 12 (Q1–Q3 11–14 cm/s) versus conduit 25 (Q1–Q3 17–31 cm/s), $P < 0.001$), resulting in a median IVC–conduit velocity mismatch of 1.8 (Q1–Q3 1.5–2.4), further augmenting during inspiration (median 2.3, Q1–Q3 1.8–3.0). IVC–conduit mismatch was inversely related to measured conduit size and positively correlated with conduit flow. The normalized IVC–conduit velocity mismatch factor during expiration and the entire respiratory cycle correlated with peak VO_2 ($r = -0.37$, $P = 0.014$ and $r = -0.31$, $P = 0.04$, respectively).

CONCLUSIONS: Important blood flow accelerations are observed from the IVC towards the conduit in adolescent Fontan patients, which is related to peak VO_2 . This study, therefore, raises concerns that implanted 16–20mm conduits have become undersized for older Fontan patients and future studies should clarify its effect on long-term outcome.

Keywords: Fontan • Hepatic venous flow • Mismatch • Extracardiac conduit • Respiration • Stenosis

ABBREVIATIONS

CSA	Cross-sectional area
HV	Hepatic venous
IVC	Inferior vena cava
SVC	Superior vena cava
TCPC	Total CavoPulmonary Connection

INTRODUCTION

The Fontan procedure provides a palliative solution for single-ventricle patients, by connecting both the superior vena cava (SVC) and inferior vena cava (IVC) directly to the pulmonary arteries [i.e. Total CavoPulmonary Connection (TCPC)]. Nowadays, most centres complete the TCPC by connecting the IVC to the right pulmonary artery (PA) using a Goretex extracardiac conduit at an age of 2–4 years [1]. However, the lack of growth potential remains concerning for older Fontan patients. To date, optimal conduit size for adult Fontan patients is unknown as no clear definition is available to describe the haemodynamic adequacy of extracardiac conduits during follow-up, beyond identifying a distinct stenosis within the Fontan conduit.

The extracardiac conduit directs 65–70% of total systemic venous return towards the PAs [2]. Since blood flow resistance is inversely related to the fourth power of the vessel radius (law of Hagen-Poiseuille), an undersized conduit leads to reduced TCPC flow efficiency [3–5]. Exercise performance has been associated with conduit size [6, 7], which is related to TCPC flow efficiency [3, 8]. On top of that, TCPC flow efficiency has been associated with the degree of liver fibrosis, a common complication in Fontan-palliated patients [9].

Recently, the *IVC–conduit velocity mismatch factor* has been proposed as a marker of conduit adequacy, describing the change in mean velocity from the subhepatic IVC towards the conduit [10]. In that study, 4D flow MRI revealed important blood flow acceleration at the level of the conduit that was associated with increased viscous energy losses resulting in less efficient TCPC blood flow [10]. Since conduit flow changes along the respiratory cycle due to intrathoracic pressure changes, evaluation of the IVC–conduit velocity mismatch along the respiratory

cycle may reveal important insights in the adequacy of the conduit size during both inspiration (highest flow) and expiration (lowest flow).

The hypothesis is that adolescent Fontan patients may outgrow implanted conduit size, leading to an increased blood flow velocity from the subhepatic IVC towards the conduit. Therefore, the aim is to assess conduit adequacy along the respiratory cycle by evaluating the IVC–conduit velocity mismatch factor using real-time 2D flow MRI and determine its relationship with exercise performance.

MATERIALS AND METHODS

Study population

Fontan patients with an extracardiac Goretex conduit prospectively underwent MRI between 2018 and 2020 at the Leiden University Medical Center, Leiden, the Netherlands. All patients >8 years old without contraindications for MRI were eligible for inclusion. The study was approved by the medical ethical review board of the hospital. Written informed consent was obtained from all patients and/or their parents.

Magnetic resonance imaging

MRI acquisition details are presented in [Supplementary Material, Table S1](#). Real-time 2D phase-contrast MRI measurements were obtained at the level of the subhepatic IVC [below entry of the hepatic venous (HV)], the extracardiac conduit and the SVC (Fig. 1A). HV flow was indirectly determined by subtracting IVC flow from conduit flow. Measurements consisted of 250 real-time [non-electro cardiogram (ECG)-gated] flow acquisitions with a sample rate of ~ 15 fps. The respiratory signal was continuously monitored using an air-filled abdominal belt. Flow rate (Q), mean velocity (V) and cross-sectional area (CSA) of each vessel were acquired by manual segmentation of the vessel lumen on all phase-contrast images (Fig. 1B, Mass software, Leiden, the Netherlands). The mean CSA during the entire flow acquisition is reported.

The workflow of the real-time 2D flow MRI analysis is shown in Fig. 1 and [Supplementary Material S1](#). Typically, 2–4

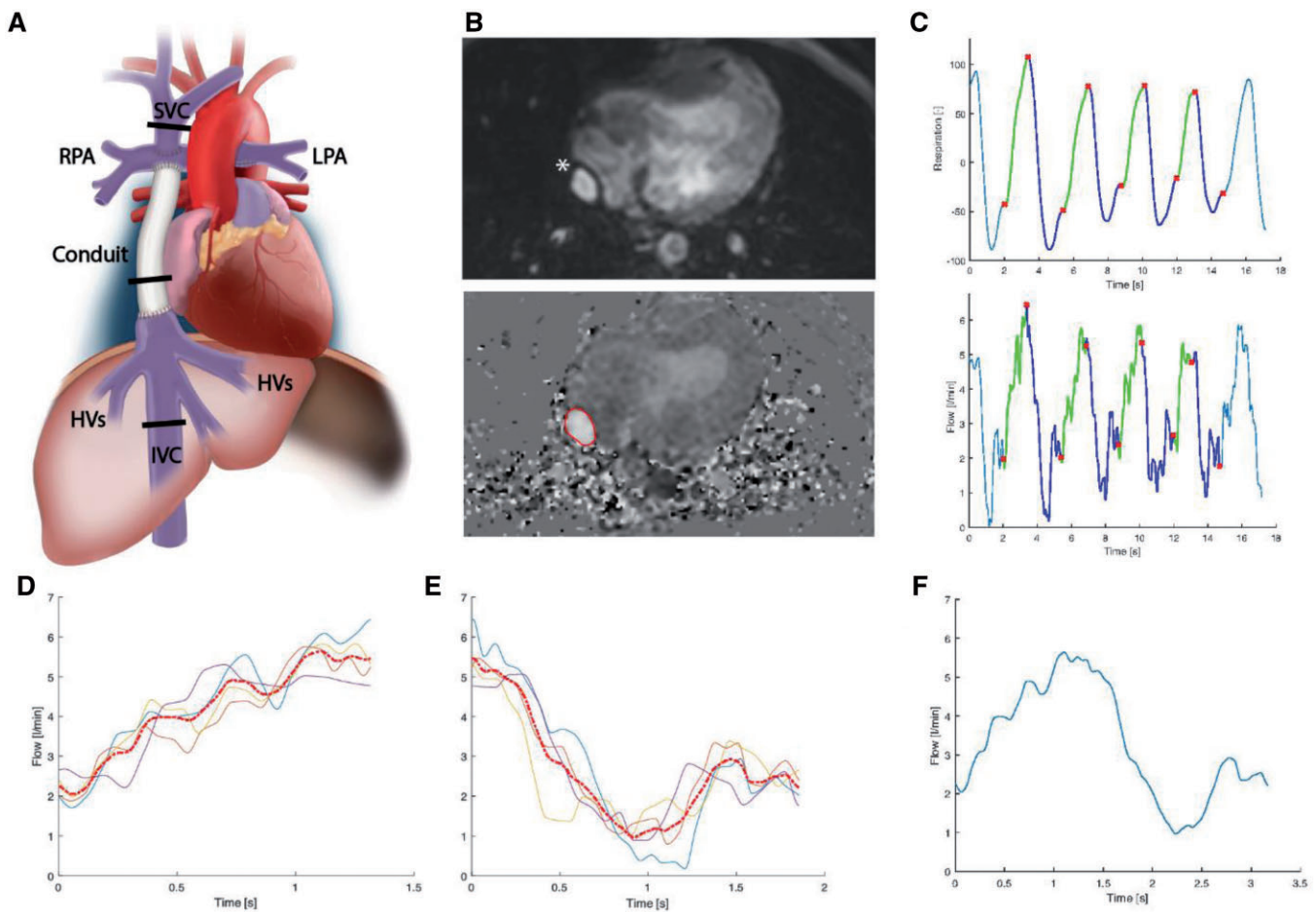


Figure 1: The workflow of the real-time 2D flow MRI analysis of a conduit flow, measurement. The same analysis is applied to the subhepatic inferior vena cava and superior vena cava. The position of the 2D flow planes are shown (A). The lumen of the conduit (*) was manually delineated on the phase-contrast images. (B) Multiple consecutive respiratory curves and corresponding flow curves (C) were automatically divided into multiple inspiration (green) and expiration (blue) parts. After interpolation, a single average curve was generated from the individual inspiratory (D) and expiratory (E) curves and subsequently combined to acquire the average respiratory cycle (F).

consecutive respiratory cycles and associated flow and velocity curves were automatically cut into inspiration and expiration phases using in-house developed software (Fig. 1C). A single flow curve was derived (Fig. 1D–F) from the average inspiratory and expiratory flow curves, which was used for the analysis of the flow parameters. To determine real-time HV flow, inspiratory and expiratory flow curves from the IVC and conduit were aligned and subsequently subtracted.

Mean flowrates and velocities (V) were determined during the entire respiratory cycle, inspiration and expiration. The ratio between mean inspiratory and mean expiratory flowrates was calculated as a marker of respiration-driven pulsatility ($Q_{\text{insp}}/Q_{\text{exp}}$). Retrograde flow fraction was calculated by dividing retrograde flow volume (retrograde flow rate \times duration of retrograde flow) by antegrade flow volume.

IVC–conduit velocity mismatch factor

The IVC–conduit velocity mismatch factor was determined for the average respiratory cycle, inspiration and expiration phases as follows: $V_{\text{conduit}}/V_{\text{IVC}}$, where V is the mean velocity in the conduit and subhepatic IVC, respectively. A mismatch factor of 1 represents equal mean velocity (ideal), <1 represents a decrease

in mean velocity (oversized conduit) and >1 represents an increase in mean velocity (undersized conduit).

The relation between the IVC–conduit velocity mismatch factor and mean conduit flow rates was analysed by grouping patients in tertiles of measured conduit CSA: $<209 \text{ mm}^2$ ($n=16$), $209\text{--}241 \text{ mm}^2$ ($n=17$) and $>241 \text{ mm}^2$ ($n=17$). Grouping patients on measured conduit size rather than on implanted conduit size is based on observations that conduit CSA can variably decrease after implantation due to neointima formation and conduit stretching [7, 11, 12]. To put CSA values in perspective to implanted conduit diameters, the theoretical CSA corresponding to 16–20-mm circular conduits is 201 mm^2 (16 mm), 254 mm^2 (18 mm) and 314 mm^2 (20 mm). Furthermore, vessel CSA normalized for the average flow rate during the respiratory cycle in each vessel is presented. To compare IVC–conduit velocity mismatch between measured conduit size groups, values were normalized for indexed conduit flow rate ($\text{l}/\text{min}/\text{m}^2$).

Cardiopulmonary exercise testing

Cardiopulmonary exercise testing was performed on an upright bicycle ergometer (GE Healthcare, Wisconsin, USA). A continuous incremental bicycle protocol was executed according to the

Godfrey protocol. Patients had to maintain a pedalling rate of 60 revolutions/min and were encouraged to cycle to exhaustion. Peak VO_2 (ml/kg/min) was determined in all patients with a respiratory exchange ratio >1.0 .

Statistical analysis

Data were presented as median (Q1–Q3) or mean (standard deviation). Normal distributions of continuous data were tested using the Shapiro–Wilk test. Correlation analysis was performed using Pearson or Spearman correlation (weak 0.3–0.5, moderate 0.5–0.7, strong ≥ 0.7 –0.9 and very strong >0.9). Measurements between the different vessels were compared using a paired t-test or Wilcoxon signed-rank test. Comparison of normalized mismatch factor between measured conduit size tertiles were performed using the Kruskal–Wallis test (adjusted for multiple comparisons using Bonferroni). A *P*-value of <0.05 was considered statistically significant. Data were analysed with SPSS 25.0 (IBM Corp., Armonk, NY, USA) and Graphpad Prism 8.0 (GraphPad Software, La Jolla, CA, USA).

RESULTS

Fifty-seven extracardiac conduit Fontan patients underwent MRI examination. Seven patients with incomplete 2D real-time MRI examinations were excluded from analysis. Patient characteristics are provided in Table 1. Cardiopulmonary exercise testing was performed in 47/50 patients, with 44 patients reaching maximal effort [median time between cardiopulmonary exercise testing and MRI 0 days (Q1–Q3 0–15 days)].

Cross-sectional area

IVC and conduit CSA were a median of 244 mm² (Q1–Q3 203–265) and 221 mm² (Q1–Q3 201–255), respectively. CSA decreased from the subhepatic IVC towards the conduit with a median of 9% (IQR -18 to 15), with IVC CSA exceeding conduit CSA in 30 patients (60%). Median normalized conduit CSA (66 mm²/l/min, Q1–Q3 54–97) was smaller compared to normalized IVC CSA (129 mm²/l/min, Q1–Q3 118–148, $P < 0.001$), decreasing a median of 44% (Q1–Q3 33–58% decrease).

Measured conduit CSA of implanted 16–20-mm conduits was 101% (Q1–Q3 93–109%), 97% (Q1–Q3 88–108%) and 94% (Q1–Q3 70–96%) of theoretical expected conduit CSA, respectively. Of note, measured conduit CSA exceeded the theoretically expected conduit CSA in some patients, which can be explained by methodological reasons (see Limitations section). In 2/6 patients with a 20-mm conduit, measured conduit CSA was 232 and 192 mm², 27% and 39% decreased compared to expected theoretical conduit CSA. The median measured conduit CSA after subdividing the patients in tertiles were per group 191 mm² (Q1–Q3 172–201), 220 mm² (Q1–Q3 214–228) and 277 mm² (Q1–Q3 251–302), respectively.

Flow

Along the entire respiratory cycle, flow rates increased from the IVC (median 1.9, Q1–Q3 1.5–2.2 l/min) towards the conduit (median 3.3, Q1–Q3 2.5–4.0 l/min, $P < 0.001$, Table 2) because of

Table 1: Patient characteristics

Male/female, <i>n</i>	24/26
Primary diagnosis, <i>n</i> (%)	
TA	12 (24)
HLHS	10 (20)
DILV + TGA	10 (20)
DORV	6 (12)
uAVSD	4 (8)
ccTGA	4 (8)
PA + IVS	2 (4)
Others	2 (4)
Dominant ventricle	
Left, <i>n</i> (%)	29 (58)
Right, <i>n</i> (%)	16 (32)
Biventricular/indeterminate, <i>n</i> (%)	5 (10)
Characteristics at Fontan procedure	
Age at Fontan, years	3.7 (1.9)
Implanted conduit size (16/18/20 mm), <i>n</i>	26/18/6
Height, cm	99 (11)
Weight, kg	15.0 (2.9)
BSA, m ²	0.64 (0.09)
Characteristics at time of MRI	
Age at MRI, years	16.9 (4.5)
Height, cm	167 (11)
Weight, kg	57 (14)
BSA, m ²	1.62 (0.24)
Time between Fontan and MRI, years	13.2 (4.1)
NYHA class I–II, <i>n</i> (%)	50 (100)
CPET	
Peak VO_2 (<i>n</i> = 44), ml/kg/min	26.4 (5.6)

Values are reported as mean (SD) unless otherwise specified.

(cc)TGA: (congenital corrected) transposition of the great arteries; BSA: body surface area; CPET: cardiopulmonary exercise testing; DILV: double inlet left ventricle; DORV: double outlet right ventricle; HLHS: hypoplastic left heart syndrome; MRI: magnetic resonance imaging; NYHA: New York Heart Association; PA + IVS: pulmonary atresia with intact ventricular septum; SD: standard deviation; TA: tricuspid atresia; uAVSD: unbalanced atrioventricular septal defect.

entry of HV flow [median increase 77% (Q1–Q3 59–104%)]. HV flow was strongly dependent on respiration, with a median $Q_{\text{insp}}/Q_{\text{exp}}$ ratio of 3.0 (Q1–Q3 2.2–4.1). During inspiration, expiration and the entire respiratory cycle, respectively, 57% (Q1–Q3 50–60), 30% (Q1–Q3 21–39) and 43% (Q1–Q3 37–51) of total conduit flow originated from the HVs.

The median $Q_{\text{insp}}/Q_{\text{exp}}$ ratio was 1.2 (Q1–Q3 1.1–1.4) in the SVC, 1.1 (Q1–Q3 1.0–1.3) in the IVC and 1.7 (Q1–Q3 1.5–2.1) in the conduit. Therefore, most pulsatility observed in the conduit originates from the pulsatile HV flow. Retrograde flow was negligible at the level of the conduit, SVC and IVC in all patients, but occurred in the HVs in 43 (86%) patients, exclusively in (early) expiration.

IVC–conduit velocity mismatch

Mean velocities in the IVC and SVC were generally low (range 10–14 cm/s) during all respiratory phases (Table 2). The combination of a decrease in CSA and an increase in flow rate resulted in higher mean velocity in the conduit compared to the IVC ($P < 0.001$ for all respiratory phases). The median IVC–conduit velocity mismatch factor during the entire respiratory cycle was 1.8 (Q1–Q3 1.5–2.4), indicating a 1.8-fold increase of the mean velocity from the subhepatic IVC towards the conduit.

Table 2: Subhepatic inferior vena cava, hepatic venous, conduit and superior vena cava characteristics

Cross-sectional area (mm ²)	Absolute CSA (mm ²)	Normalized CSA		Q _{insp} /Q _{exp} ratio
		(mm ² per l/min)		
Flow (l/min)	Entire respiratory cycle	Inspiration	Expiration	
Mean velocity (cm/s)	Entire respiratory cycle	Inspiration	Expiration	
IVC	244 (203 to 265)	129 (118 to 148)		
Conduit	221 (201 to 255)	66 (54 to 97)		
SVC	218 (161 to 256)	150 (129 to 197)		
Change in CSA from IVC to conduit, %	-9 (-18 to 15)	-44 (-58 to -33)		
IVC	1.9 (1.5 to 2.2) ^{†,‡}	2.1 (1.6 to 2.5) ^{†,§}	1.7 (1.3 to 2.1) ^{†,§}	1.1 (1.0 to 1.3)
HV	1.5 (1.0 to 1.8) ^{†,‡}	2.6 (2.1 to 3.1) ^{†,§}	0.7 (0.5 to 1.2) ^{†,§}	3.0 ^a (2.2 to 4.1)
Conduit	3.3 (2.5 to 4.0) ^{†,‡}	4.5 (3.9 to 5.3) ^{†,§}	2.6 (1.9 to 3.3) ^{†,§}	1.7 (1.5 to 2.1)
SVC	1.3 (1.1 to 1.6) ^{†,‡}	1.5 (1.3 to 1.8) ^{†,§}	1.2 (1.0 to 1.5) ^{†,§}	1.2 (1.1 to 1.4)
Change in flow from IVC to conduit, %	77 (59 to 104) ^{†,‡}	131 (99 to 152) ^{†,§}	44 (27 to 65) ^{†,§}	
Contribution of HV flow to conduit flow, %	43 (37 to 51) ^{†,‡}	57 (50 to 60) ^{†,§}	30 (21 to 39) ^{†,§}	
Retrograde-to-antegrade flow ratio IVC, %	0 (0 to 0)	0 (0 to 0)	0 (0 to 0)	
Retrograde-to-antegrade flow ratio HV, %	5 (1 to 9) ^{†,‡}	0 (0 to 0) ^{†,§}	13 (3 to 31) ^{†,§}	
Retrograde-to-antegrade flow ratio conduit, %	0 (0 to 0)	0 (0 to 0)	0 (0 to 0)	
Retrograde-to-antegrade flow ratio SVC, %	0 (0 to 0)	0 (0 to 0)	0 (0 to 0)	
IVC	12 (11 to 14) ^{†,‡}	13 (12 to 16) ^{†,§}	12 (10 to 14) ^{†,§}	
Conduit	25 (17 to 31) ^{†,‡}	35 (25 to 40) ^{†,§}	19 (12 to 25) ^{†,§}	
SVC	11 (9 to 13) ^{†,‡}	13 (10 to 15) ^{†,§}	10 (8 to 12) ^{†,§}	
IVC-conduit velocity mismatch factor	1.8 (1.5 to 2.4) ^{†,‡}	2.3 (1.8 to 3.0) ^{†,§}	1.5 (1.2 to 2.1) ^{†,§}	

Values are reported as median (Q1-Q3).

CSA: cross-sectional area; HV: hepatic venous; IVC: inferior vena cava; SVC: superior vena cava.

^aThree cases with negative ratios were excluded.

[†]P-value <0.001 compared to inspiration.

[‡]P-value <0.001 compared to expiration.

[§]P-value <0.001 compared to the entire respiratory cycle.

Because of the important respiratory dependency of HV flow, IVC-conduit velocity mismatch was higher during inspiration (median 2.3, Q1-Q3 1.8-3.0, $P < 0.001$) and lower during expiration (median 1.6, Q1-Q3 1.2-2.1, $P < 0.001$, Fig. 2 and Video 1) compared to the entire respiratory cycle. A moderate positive correlation was found between mean conduit flow rate and the IVC-conduit velocity mismatch factor during the entire respiratory cycle ($r = 0.58$), inspiration ($r = 0.42$) and expiration ($r = 0.69$, Fig. 3). Highest mismatch was present in the group with smallest conduits (group 1 <209 mm², Figs. 3 and 4). Up to a 4.4-fold increase in mean velocity was observed during inspiration in group 1 patients with high flow rates (Fig. 3B). Importantly, only 5 patients (10%) had a mismatch factor <1 during expiration indicating flow expansion due to an relatively oversized conduit (all in groups 2-3, age 10-14 years, Fig. 3B). The normalized IVC-conduit velocity mismatch factor during expiration and the entire respiratory cycle correlated with peak VO₂ ($r = -0.37$, $P = 0.014$ and $r = -0.31$, $P = 0.04$, respectively).

A moderate positive correlation was found between BSA and mean conduit flow during all respiratory phases ($r = 0.62-0.70$), with considerable variation in flow rates between patients with similar body sizes (Supplementary Material, Fig. S1). No correlation was found between IVC mean velocity and BSA ($r = 0.26$, $P = 0.06$).

DISCUSSION

This study evaluated the haemodynamic adequacy of implanted 16-20-mm extracardiac conduit sizes along the respiratory cycle

at a mean interval of 13 years after Fontan completion. The main findings show that at a mean age of 17 years, absolute conduit CSA is 9% smaller as compared to the CSA of the subhepatic IVC, even though all HV flow still needs to enter the IVC. Consequently, important blood flow accelerations (IVC-conduit velocity mismatch) are present from the subhepatic IVC towards the conduit which are further augmented during inspiration. The normalized IVC-conduit mismatch factor during expiration and the entire respiratory cycle inversely correlated with peak VO₂. This study raises concerns that implanted 16-20-mm conduits have become undersized for adolescent Fontan patients.

Currently, typically 16-20-mm conduits are implanted in a 'one size fits all approach', with all children receiving approximately the same conduit size despite different projected adult body size and related flow conditions. Itatani *et al.* recommended 16-18-mm conduits for 2-3 year old patients based on evaluation of energy loss and flow stagnation using computational fluid dynamics in young Fontan patients (mean BSA 0.5, 3.0 years old, mean conduit flow 0.85 l/min). Conduit size recommendations for older Fontan patients could therefore not be determined. In comparison, in our study BSA and conduit flow rates were ~3-4 times higher. In a recent expert review, implantation of 16-18-mm conduits are recommended, with larger conduit sizes being associated with worse exercise capacity [6, 13]. However, late studies evaluating haemodynamics of these conduit sizes in older Fontan patients are currently lacking. The proposed adequacy of 16-20-mm conduit sizes for adult Fontan patients has also been based on IVC diameters in healthy adults [12, 14]. Interestingly, the subhepatic IVC diameter is already in the order of 18 mm in healthy adults [15]. The mean suprahepatic

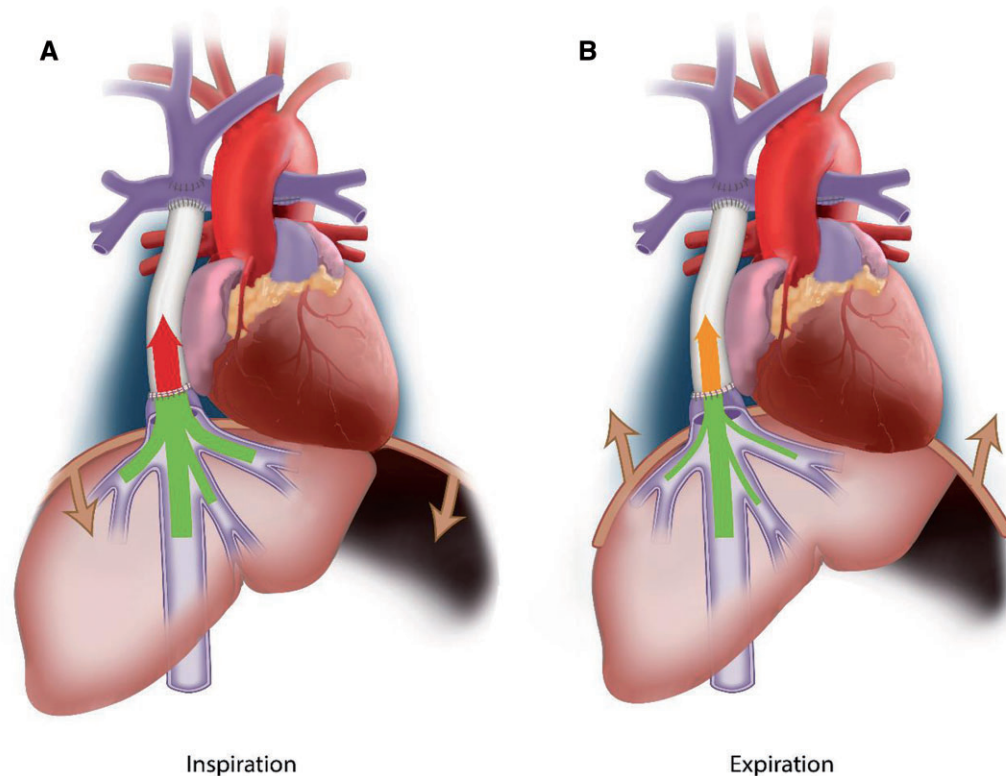
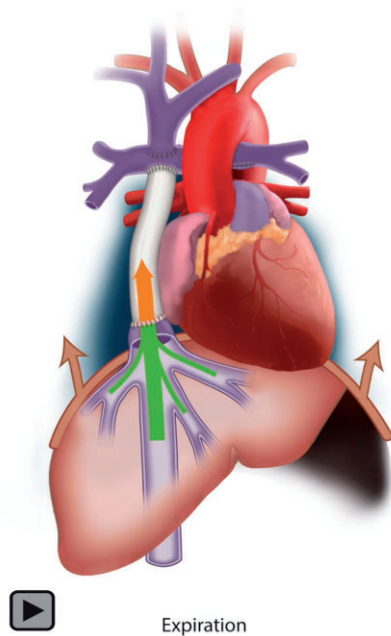


Figure 2: The presence of inferior vena cava–conduit velocity mismatch is schematically shown during inspiration (A) and expiration (B). The thickness of the arrow indicates the amount of flow and the colour indicates the blood flow velocity. An important increase in mean velocity is observed from the subhepatic inferior vena cava towards the conduit in both inspiration (highest mismatch) and expiration.



Video 1: The presence of inferior vena cava–conduit velocity mismatch is schematically shown during inspiration (A) and expiration (B). The thickness of the arrow indicates the amount of flow and the colour indicates the blood flow velocity. An important increase in mean velocity is observed from the subhepatic inferior vena cava towards the conduit in both inspiration (highest mismatch) and expiration.

IVC diameter, distal to entry of the HVs, is significantly larger to account for the increase in flow rate caused by the HVs; a mean of 24 mm (CSA 452 mm²) in healthy adults [16], 27 mm (CSA 572 mm²) in adults with congenital heart disease [16] and up to even 770 mm² in adult Fontan patients [17]. In our study, median conduit CSA was only 221 mm² and a median 9% smaller compared to the subhepatic IVC CSA, indicating that implanted conduits have become undersized. This is a result of both somatic growth leading to increased flow rates and CSA of surrounding vessels, but also by a decrease in actual conduit CSA during follow-up due to stretching/neo-intima formation in some patients [7, 11, 12]. Congestion most likely did not play a role in the size of the IVC, as no negative correlation was found between BSA and IVC mean velocity.

Previously, our group published the concept of IVC–conduit velocity mismatch based on observations using 4D flow MRI [10]. This parameter is based on the concept that both flow expansion (decrease in velocity) and flow contraction (increase in velocity) should ideally be absent to avoid increased energy loss and/or thrombosis risk [18]. Indeed, mean velocities remained in a relatively narrow range in the native subhepatic IVC and SVC, indicating that these vessels adapt to change in flow rates over time. The rigid extracardiac conduit lacks this physiologic adaptation, explaining the increase in mean conduit velocity with higher conduit flow rates. This becomes evident when looking at the vessels CSA normalized for flow, which was a median 44% smaller for the conduit compared to the IVC. Importantly, IVC–conduit velocity mismatch >1 was already present during expiration in 90% of patients, furthermore indicating that these conduits have

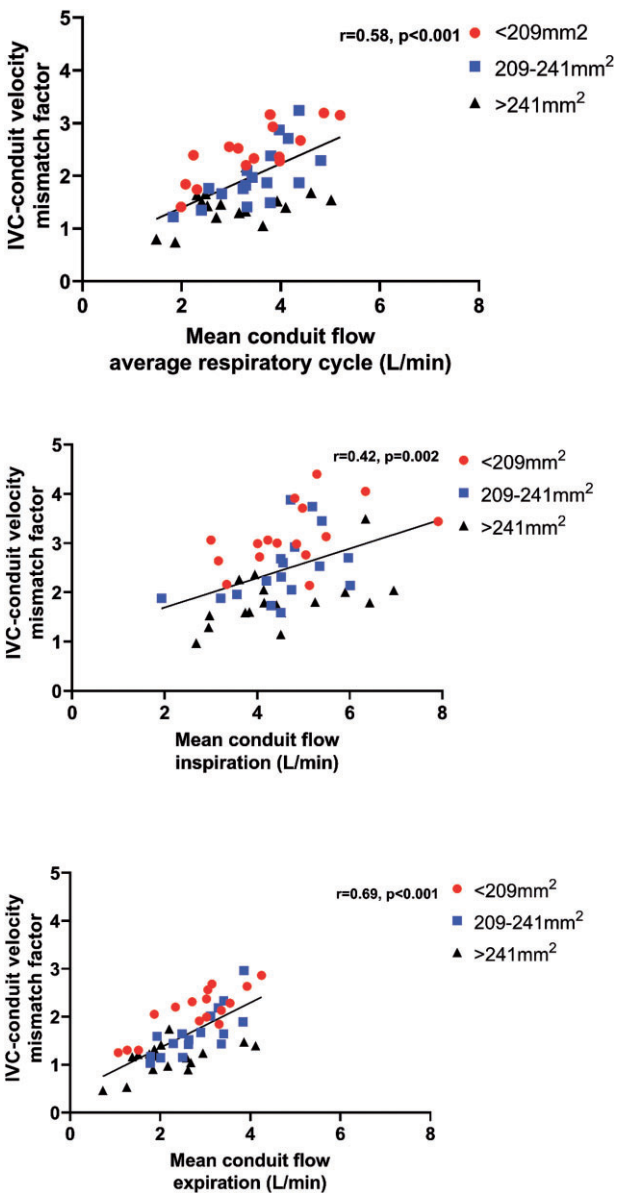


Figure 3: The correlation between conduit flow rate and inferior vena cava-conduit velocity mismatch factor is shown for the entire respiratory cycle (A), inspiration (B) and expiration (C). Patients are colour-coded into 3 groups based on the measured conduit size for visualization purposes only.

become relatively undersized even during the respiratory phase with lowest flow rates.

In light of the reported normal suprahepatic IVC diameters in healthy adults, it is not surprising that we observed a median mismatch factor of 1.8, as median conduit size was only 221 mm². Since $Q = V \times A$ (where Q is the flow rate, V is the mean velocity and A is the CSA), conduit CSA must theoretically be a 1.8-fold higher in our cohort to avoid an increase in mean velocity, effectively indicating a long-segmental stenosis of approximately 50%. These projected values would be in line with the CSA of the suprahepatic IVC observed in healthy persons [16]. Interestingly, the CSA of an intra-atrial lateral Fontan tunnel, in which part of the tunnel wall consists of atrial tissue with growth potential, is already 420–580 mm² (23–27 mm) at an age of 10–15 years [19, 20]. Thus, the physiologic response to increased flow

rates during somatic growth seems to lead to importantly larger intra-atrial Fontan tunnels compared to the rigid extracardiac conduit.

Clinical relevance: TCPC efficiency and long-term outcome

The observed IVC-conduit velocity mismatch may be of clinical relevance, as the conduit plays an important role in TCPC haemodynamics. Efficient and unobstructed TCPC blood flow with minimal energy loss is desired to minimize the elevation in CVP while ensuring optimal preload in Fontan patients [5, 21]. On average, 65–70% of total systemic venous return enters the TCPC via the conduit, further increasing to 79% during lower-leg exercise [2]. Since blood flow resistance is inversely proportional to the fourth power of the vessel radius (law of Hagen-Poiseuille), undersized conduits are among the most important factors of TCPC resistance [3]. In a large study of CFD simulations during resting conditions, patients with small Fontan conduits showed a three-fold higher TCPC resistance compared to the mean resistance of the entire study cohort, potentially reaching values up to 35–50% of normal pulmonary vascular resistance [5]. TCPC resistance further increases exponentially during exercise [22] while pulmonary vascular resistance decreases during exercise [23], making TCPCs with a relatively undersized conduit a potential bottleneck in the Fontan circulation [4, 24].

Decreased TCPC flow efficiency is associated with reduced preload and thereby cardiac output, associated with a decreased exercise capacity [5, 21, 25]. Our study showed a weak inverse correlation between the normalized IVC-conduit velocity mismatch factor and peak VO_2 , which might be explained by the increased TCPC resistance in patients with smaller conduits with higher mismatch. This is in line with recent findings by Patel *et al.*, who found a correlation between minimum conduit size and predicted peak VO_2 [7].

The increased resistance caused by undersized conduits will lead to an elevated central venous pressure (CVP) to maintain cardiac output, which plays an important role in the pathophysiology of protein losing enteropathy and liver cirrhosis. Fontan patients with an extracardiac conduit show a faster progression of liver fibrosis compared to intra-atrial tunnel Fontan patients [26]. We speculate that the presence of undersized conduits showing important IVC-conduit velocity mismatch might be one of the reasons by increasing afterload for HV flow, especially during inspiration. The acceleration of blood flow in the conduit may also have adverse effects on downstream energy-consuming flow patterns (e.g. vortices, helices) or caval flow collision within the Fontan confluence, further decreasing TCPC flow efficiency [24].

Potential implications for surgical strategy

Our current practice is to implant 18 mm fenestrated conduits in our patients and since long we have abandoned implanting 16 mm conduits. However, this study shows that a strategy of implanting rigid conduits in children aged 2–4 years results in suboptimal haemodynamics at older age and is therefore not ideal. As implantation of larger conduit sizes in young children is unfeasible by anatomical constraints as well as undesirable as they will cause sluggish flow increasing thrombosis risk [14, 18], we believe that conduits of other materials should be considered rather than implanting larger conduits. Currently, stretchable ePTFE grafts (PECALabs) are

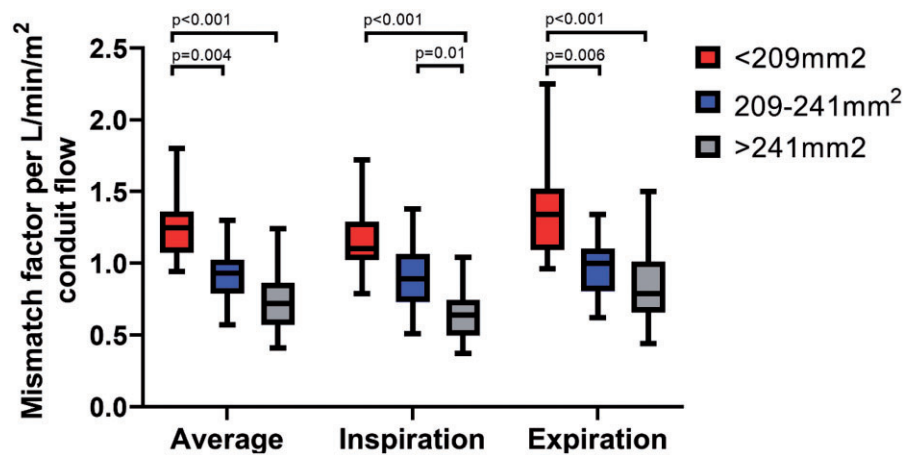


Figure 4: The inferior vena cava–conduit velocity mismatch factor normalized for conduit flow rate per BSA is shown for the average respiratory cycle, inspiration and expiration for the 3 groups of measured conduit size. For example, a normalized inferior vena cava–conduit mismatch factor of 0.5 means an increase in velocity from the inferior vena cava towards the conduit when conduit flow rate is $>2\text{ l/min/m}^2$.

available which could potentially minimize the decrease in conduit CSA caused by stretching during somatic growth and can be dilated to some extent when the child becomes older. Furthermore, tissue-engineered conduits are being developed and may be promising by allowing for growth [27].

Based on the current study, it is impossible to speculate which levels of IVC–conduit velocity mismatch warrants replacement of the conduit. It will be important to know how observed IVC–conduit velocity mismatch relates to haemodynamic markers such as pressure drop and resistance and how the mismatch develops over time, which will be essential information for clinical decision-making about possible intervention. Essentially any pressure drop from the caval veins towards the PAs is undesirable and pressure gradients as low as $\pm 1\text{ mmHg}$ already may form an indication to intervene, although exact cut-off points are not available at this moment. Furthermore, although our cohort represented relatively asymptomatic patients without signs of Fontan failure, the chronic negative effects of IVC–conduit velocity mismatch may only become apparent later in life. Serial studies with comprehensive MRI flow evaluation and longer follow-up are needed to determine the effect of undersized conduits on long-term outcome.

Limitations

Flow rates were analysed along the respiratory cycle only, irrespective of the phase of the cardiac cycle. Since flow pulsatility along the cardiac cycle is only minimal [28] and predominantly is determined by the respiratory cycle [29], inaccuracies are likely small. Furthermore, CSA was measured from 2D real-time PC-MRI which has a limited spatial resolution and can overestimate CSA when the flow acquisition is not planned precisely perpendicular to the vessel lumen. However, these errors are likely systematic as CSA of all vessels were measured using the same method. HV flow was only measured indirectly by subtracting IVC flow from conduit flow, but results are in strong agreement with a previous study that directly measured HV flow using echocardiography [30].

CONCLUSION

This study evaluated the haemodynamic adequacy of extracardiac Goretex conduits sized 16–20 mm along the respiratory

cycle in Fontan patients. Important IVC–conduit velocity mismatch, i.e. an increase in velocity from the subhepatic IVC towards the conduit, is observed at a mean interval of 13 years after Fontan completion. This raises concerns that implanted 16–20-mm conduits have become undersized for older Fontan patients. The normalized IVC–conduit velocity mismatch factor showed an inverse weak correlation with peak VO_2 . Future studies are warranted to clarify the long-term effect of IVC–conduit velocity mismatch on clinical outcome.

SUPPLEMENTARY MATERIAL

Supplementary material is available at *EJCTS* online.

ACKNOWLEDGEMENTS

The authors gratefully thank Ronald Slagter for the illustrations in Figs. 1A and 2.

Funding

Friso M. Rijnberg is funded by a grant from Stichting Hartekind and by the Dutch Heart Foundation (2018-T083).

ETHICS APPROVAL AND CONSENT TO PARTICIPATE

The study was approved by the medical ethical review board of the Leiden University Medical Center. Written informed consent was obtained from all patients and/or their parents.

Conflict of interest: none declared.

Data Availability Statement

The datasets used and/or analysed during the current study are available from the corresponding author on reasonable request.

Author contributions

Friso M. Rijnberg: Conceptualization; Data curation; Formal analysis; Investigation; Methodology; Visualization; Writing—original draft. **Séline F.S. van der Woude:** Formal analysis; Methodology; Software; Writing—review & editing. **Mark G. Hazekamp:** Supervision; Writing—review & editing. **Pieter J. van den Boogaard:** Data curation; Investigation. **Hildo J. Lamb:** Resources; Writing—review & editing. **Covadonga Terol Espinosa de Los Monteros:** Formal analysis; Writing—review & editing. **Lucia J.M. Kroft:** Resources; Writing—review & editing. **Sasa Kenjeres:** Writing—review & editing. **Tawab Karim:** Formal analysis; Methodology; Software; Writing—review & editing. **Monique R.M. Jongbloed:** Writing—review & editing. **Jos J.M. Westenberg:** Funding acquisition; Investigation; Methodology; Resources; Supervision; Writing—review & editing. **Jolanda J. Wentzel:** Conceptualization; Writing—review & editing. **Arno A.W. Roest:** Funding acquisition; Methodology; Supervision; Writing—review & editing.

Reviewer information

European Journal of Cardio-Thoracic Surgery thanks the anonymous reviewer(s) for their contribution to the peer review process of this article.

REFERENCES

- [1] Rychik J, Atz AM, Celermajer DS, Deal BJ, Gatzoulis MA, Gewillig MH *et al.*; On behalf of the American Heart Association Council on Cardiovascular Disease in the Young and Council on Cardiovascular and Stroke Nursing. Evaluation and management of the child and adult with Fontan circulation: a scientific statement from the American Heart Association. *Circulation* 2019;140:CIR0000000000000696.
- [2] Hjortdal VE, Emmertsen K, Stenbøg E, Fründ T, Schmidt MR, Kromann O *et al.* Effects of exercise and respiration on blood flow in total cavopulmonary connection: a real-time magnetic resonance flow study. *Circulation* 2003;108:1227–31.
- [3] Tang E, Restrepo M, Haggerty CM, Mirabella L, Bethel J, Whitehead KK *et al.* Geometric characterization of patient-specific total cavopulmonary connections and its relationship to hemodynamics. *JACC Cardiovasc Imaging* 2014;7:215–24.
- [4] Rijnberg FM, Hazekamp MG, Wentzel JJ, de Koning PJH, Westenberg JJM, Jongbloed MRM *et al.* Energetics of blood flow in cardiovascular disease: concept and clinical implications of adverse energetics in patients with a Fontan circulation. *Circulation* 2018;137:2393–407.
- [5] Haggerty CM, Restrepo M, Tang E, de Zelicourt DA, Sundareswaran KS, Mirabella L *et al.* Fontan hemodynamics from 100 patient-specific cardiac magnetic resonance studies: a computational fluid dynamics analysis. *J Thorac Cardiovasc Surg* 2014;148:1481–9.
- [6] Lee SY, Song MK, Kim GB, Bae EJ, Kim SH, Jang SI *et al.* Relation between exercise capacity and extracardiac conduit size in patients with Fontan circulation. *Pediatr Cardiol* 2019;40:1584–90.
- [7] Patel ND, Friedman C, Herrington C, Wood JC, Cheng AL. Progression in Fontan conduit stenosis and hemodynamic impact during childhood and adolescence. *J Thorac Cardiovasc Surg* 2020;162:372–380.e2.
- [8] Khiabani RH, Whitehead KK, Han D, Restrepo M, Tang E, Bethel J *et al.* Exercise capacity in single-ventricle patients after Fontan correlates with haemodynamic energy loss in TCPC. *Heart* 2015;101:139–43.
- [9] Trusty PM, Wei ZA, Rychik J, Graham A, Russo PA, Surrey LF *et al.* Cardiac magnetic resonance-derived metrics are predictive of liver fibrosis in Fontan patients. *Ann Thorac Surg* 2020;109:1904–11.
- [10] Rijnberg FM, Elbaz MSM, Westenberg JJM, Kamphuis VP, Helbing WA, Kroft LJ *et al.* Four-dimensional flow magnetic resonance imaging-derived blood flow energetics of the inferior vena cava-to-extracardiac conduit junction in Fontan patients. *Eur J Cardiothorac Surg* 2019;55:1202–10.
- [11] Amodeo A, Galletti L, Marianeschi S, Picardo S, Giannico S, Di Renzi P *et al.* Extracardiac Fontan operation for complex cardiac anomalies: seven years' experience. *J Thorac Cardiovasc Surg* 1997;114:1020–30, discussion 30–1.
- [12] Cho S, Kim WH, Choi ES, Kwak JG, Chang HW, Hyun K *et al.* Outcomes after extracardiac Fontan procedure with a 16-mm polytetrafluoroethylene conduit. *Eur J Cardiothorac Surg* 2018;53:269–75.
- [13] Daley M, d'Udekem Y. The optimal Fontan operation: lateral tunnel or extracardiac conduit? *J Thorac Cardiovasc Surg* 2020; S0022-5223(20)33445-0. <https://doi.org/10.1016/j.jtcvs.2020.11.179>.
- [14] Alexi-Meskishvili V, Ovroutski S, Ewert P, Dahnert I, Berger F, Lange PE *et al.* Optimal conduit size for extracardiac Fontan operation. *Eur J Cardiothorac Surg* 2000;18:690–5.
- [15] Moreno FL, Hagan AD, Holmen JR, Pryor TA, Strickland RD, Castle CH. Evaluation of size and dynamics of the inferior vena cava as an index of right-sided cardiac function. *Am J Cardiol* 1984;53:579–85.
- [16] Ettinger E, Steinberg I. Angiocardiographic measurement of the cardiac segment of the inferior vena cava in health and in cardiovascular disease. *Circulation* 1962;26:508–15.
- [17] Zieliński P, Michałowska I, Kowalik E, Mierzyńska A, Klisiewicz A, Kowalczyk M *et al.* Is there any role for computed tomography imaging in anticipating the functional status in adults late after total cavopulmonary connection? A retrospective evaluation. *Kardiol Pol* 2019;77:1062–9.
- [18] Itatani K, Miyaji K, Tomoyasu T, Nakahata Y, Ohara K, Takamoto S *et al.* Optimal conduit size of the extracardiac Fontan operation based on energy loss and flow stagnation. *Ann Thorac Surg* 2009;88:565–72, discussion 72–3.
- [19] Bossers SS, Cibis M, Gijsen FJ, Schokking M, Strengers JL, Verhaart RF *et al.* Computational fluid dynamics in Fontan patients to evaluate power loss during simulated exercise. *Heart* 2014;100:696–701.
- [20] Restrepo M, Mirabella L, Tang E, Haggerty CM, Khiabani RH, Fynn-Thompson F *et al.* Fontan pathway growth: a quantitative evaluation of lateral tunnel and extracardiac cavopulmonary connections using serial cardiac magnetic resonance. *Ann Thorac Surg* 2014;97:916–22.
- [21] Sundareswaran KS, Pekkan K, Dasi LP, Whitehead K, Sharma S, Kanter KR *et al.* The total cavopulmonary connection resistance: a significant impact on single ventricle hemodynamics at rest and exercise. *Am J Physiol Heart Circ Physiol* 2008;295:H2427–35.
- [22] Whitehead KK, Pekkan K, Kitajima HD, Paridon SM, Yoganathan AP, Fogel MA. Nonlinear power loss during exercise in single-ventricle patients after the Fontan: insights from computational fluid dynamics. *Circulation* 2007;116:1165–71.
- [23] Schmitt B, Steendijk P, Ovroutski S, Lunze K, Rahmzadeh P, Maarouf N *et al.* Pulmonary vascular resistance, collateral flow, and ventricular function in patients with a Fontan circulation at rest and during dobutamine stress. *Circ Cardiovascular Imaging* 2010;3:623–31.
- [24] Rijnberg FM, van Assen HC, Hazekamp MG, Roest AAW, Westenberg JJM. Hemodynamic consequences of an undersized extracardiac conduit in an adult fontan patient revealed by 4-dimensional flow magnetic resonance imaging. *Circ Cardiovasc Imaging* 2021;14:e012612.
- [25] Goldberg DJ, Avitabile CM, McBride MG, Paridon SM. Exercise capacity in the Fontan circulation. *Cardiol Young* 2013;23:824–30.
- [26] Evans WN, Acherman RJ, Mayman GA, Galindo A, Rothman A, Winn BJ *et al.* The Rate of Hepatic Fibrosis Progression in Patients Post-Fontan. *Pediatr Cardiol* 2020;41:905–9.
- [27] Schwarz EL, Kelly JM, Blum KM, Hor KN, Yates AR, Zbinden JC *et al.* Hemodynamic performance of tissue-engineered vascular grafts in Fontan patients. *NPJ Regen Med* 2021;6:38.
- [28] Rijnberg FM, van Assen HC, Juffermans JF, Kroft LJ, van den Boogaard PJ, de Koning PJH *et al.* Reduced scan time and superior image quality with 3D flow MRI compared to 4D flow MRI for hemodynamic evaluation of the Fontan pathway. *Sci Rep* 2021;11:6507.
- [29] van der Woude SFS, Rijnberg FM, Hazekamp MG, Jongbloed MRM, Kenjeres S, Lamb HJ *et al.* The influence of respiration on blood flow in the Fontan circulation: insights for imaging-based clinical evaluation of the total cavopulmonary connection. *Front Cardiovasc Med* 2021;8:683849.
- [30] Hsia TY, Khambadkone S, Deanfield JE, Taylor JF, Migliavacca F, De Leval MR. Subdiaphragmatic venous hemodynamics in the Fontan circulation. *J Thorac Cardiovasc Surg* 2001;121:436–47.